

Article

Examination of the Effect of RF Field on Fe-MWCNTs and Their Application in Medicine

Katarzyna Wojtera ^{1,*}, Krzysztof Smółka ¹, Łukasz Szymański ¹, Sławomir Wiak ¹
and Aleksandra Urbanek ²

¹ Institute of Mechatronics and Information Systems, Lodz University of Technology, 90-537 Lodz, Poland; krzysztof.smolka@p.lodz.pl (K.S.); lukasz.szymanski@p.lodz.pl (Ł.S.); slawomir.wiak@p.lodz.pl (S.W.)

² International Faculty of Engineering, Lodz University of Technology, 90-537 Lodz, Poland; aleksandra-urbanek@wp.pl

* Correspondence: katarzyna.wojtera@dokt.p.lodz.pl

Abstract: Carbon nanotubes are a material with excellent properties, which result in a wide range of possible applications, from electronics to medicine. This paper presents the investigation of the possibility of Fe-MWCNTs' application as heating agents for targeted thermal ablation of cancer cells, which could lead to the development of an innovative cancer treatment method. The article describes the process of synthesis of multi-walled carbon nanotubes filled with iron (Fe-MWCNTs) and provides an examination of their magnetic properties. Fe-MWCNTs were synthesized by catalytic chemical vapor deposition (CCVD). Relevant properties of the nanoparticles in terms of functionalization for biomedical applications were exploited and their magnetic properties were investigated to determine the heat generation efficiency induced by exposure of the particles to an external electromagnetic field. The reaction of the samples was measured for 40 min of exposure. The results showed an increase in sample temperature that was proportional to the concentration.

Keywords: multi-walled carbon nanotubes filled with iron (Fe-MWCNTs); chemical vapor deposition (CVD); hyperthermal ablation of cells; radiofrequency (RF) electromagnetic field



check for updates

Citation: Wojtera, K.; Smółka, K.; Szymański, Ł.; Wiak, S.; Urbanek, A. Examination of the Effect of RF Field on Fe-MWCNTs and Their Application in Medicine. *Electronics* **2022**, *11*, 2099. <https://doi.org/10.3390/electronics11132099>

Academic Editors: Alessandro Gabrielli and Jonghwa Eom

Received: 31 March 2022

Accepted: 30 June 2022

Published: 5 July 2022

Publisher's Note: MDPI stays neutral with regard to jurisdictional claims in published maps and institutional affiliations.



Copyright: © 2022 by the authors. Licensee MDPI, Basel, Switzerland. This article is an open access article distributed under the terms and conditions of the Creative Commons Attribution (CC BY) license (<https://creativecommons.org/licenses/by/4.0/>).

1. Introduction

Due to their unique chemical, mechanical, electrical, and magnetic properties, carbon nanotubes have found wide applications in many industries and are a promising material to be used for many innovative solutions. Among others, carbon nanotubes can potentially be used as electrode materials in next-generation electrochemical cells or in electron technologies in next-generation computers [1]. They can be beneficially used in environmental protection due to their ability to remove dioxins that are present in chemical, medical, or municipal wastes [2]. Carbon nanotubes are also increasingly used as fillers for polymer composites. Such composites are characterized by improved mechanical properties, high electrical conductivity, and resistance to various deformations [3]. An interesting application of carbon nanotubes can be their use as “nanocontainers” [1]. Numerous free spaces enable carbon nanotubes to be filled with various chemical compounds. This, in turn, raises the possibility of using them in space technology, as 1 gram of carbon nanotubes can store as much as 20 dm³ of hydrogen [4].

Very interestingly and at the same time, the most studied application of carbon nanotubes is their use in electronics [5,6]. In new generation computers they can play a very important role in magnetic memory, which will contribute to much faster data processing and storing than if silicon blades were used [5,7]. It is possible to construct new-generation transparent electronics based on 1D metal oxide nanowires [6]. Another application of carbon nanomaterials are active fibers with electro-optic functionalities, which are promising building blocks for the emerging and rapidly growing field of fiber and textile electronics [8]. Moreover, using carbon nanotubes we are able to construct a flat-walled display in

which this material displaces molybdenum tips. Such a display is able to replace liquid crystal and plasma screens, which will be associated with an image with about a thousand times better resolution [9]. Due to the presence of micro- and macropores, we can also use them to produce supercapacitors [10]. It was found that carbon nanotubes exhibit the phenomenon of so-called Coulomb blockade [11]. The repulsive interaction that occurs between the electrons prevents more than one additional electron from being delivered to the nanotube at the same time. Due to this effect, it is possible to construct single-electrode transistors that have very high sensitivity. A carbon nanotube transistor operating at room temperature has already been successfully constructed in which a single electron causes a transition to the conduction state [12–14]. This leads to a significant reduction in radiated heat, making it possible to build future processors that are significantly faster than current ones. Other examples of the wide use of carbon nanotubes in electronics include: micro-cathodes, hyperlinks made of two connected nanotubes, illumination devices, or quantum resistors [1,13,14].

Another promising application area of carbon nanotubes could be medicine. Using carbon nanotubes, it will be possible to control the human body's response to various external stimuli, as well as stimulate the heart muscle, so the material could help save lives [15,16]. In addition, single-walled nanotubes that are filled with appropriate liquids are used as medicine dispensers. It is possible to fill nanotubes with a medicinal substance and after appropriate modification of their surface with functional groups they are recognized, e.g., by cancer cell receptors, to transport this substance directly to the diseased area [16,17]. The carrier penetrates the cell and inside the cell the drug is released [16–18]. Surface modifications of carbon nanotubes can give nanotubes a number of applications in medical diagnostics, for example, attachment of a fluorescent dye to the surface of the nanotube and appropriate functionalization can contribute to the creation of biosensors that detect diseases and disorders at a very early stage. In combination with targeted therapy, it may provide the possibility of simultaneous monitoring of the effects of a given therapy [19].

Another highly innovative and extremely significant application of carbon nanotubes, which is directly related to the subject of this article, could be to use them to selectively destroy cells (particularly cancer cells). For this purpose, CNTs filled with a ferromagnet (e.g., iron) are delivered, in a similar way to drug delivery systems, to diseased cells [20]. The nanotubes are then heated externally by thermal ablation which causes the temperature of the cell to rise and the cell to die from the excess heat [21,22]. In this way, only diseased cells can be destroyed without acting invasively on the rest of the body [20–24]. Exposure of the cells to temperatures greater than 42 °C caused cell death, because above this temperature proteins coagulate [25,26].

The research objective was to investigate the possibility of developing carbon nanotubes, which could be used in thermal ablation of cancer cells, after proper functionalization. The article describes the examination of the behavior of MWCNTs filled with iron in an RF field. The novelty of the research lies in the development and demonstration of an original method that can bring science significantly closer to solving a problem related to cancer treatment.

2. Materials and Methods

The research involved several stages. Firstly, the material was produced using an electrothermal method, then the material was purified and prepared for further testing. The material was then characterized and its iron content examined using thermogravimetric analysis. The next stage was the samples' preparation for temperature rise studies. The process diagram is shown in Figure 1.

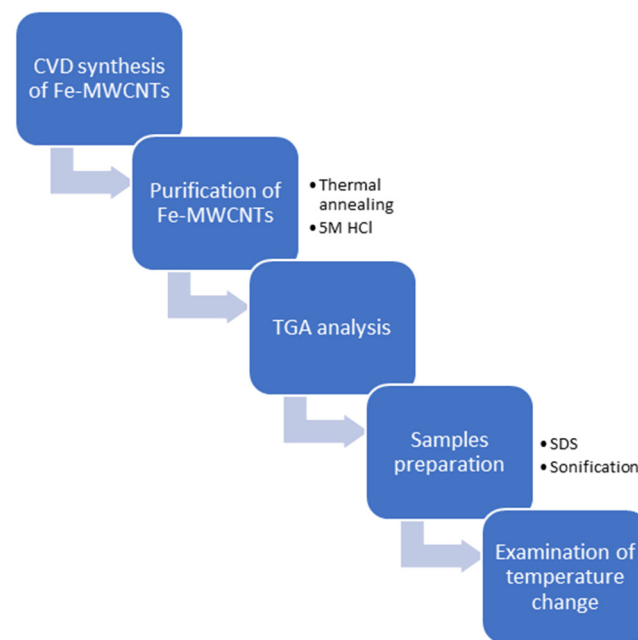


Figure 1. The examination stages diagram.

2.1. Synthesis of Fe-MWCNTs

Multi-walled iron-filled carbon nanotubes were synthesized by catalytic chemical vapor deposition (CCVD) [19,27]. The synthesis process was carried out in a three-zone furnace, which allowed independent temperature control of each zone. A quartz tube was placed inside the furnace to act as a reactor in which the synthesis of Fe-MWCNTs took place. Inside the reactor, a silicon wafer was placed in the deposition zone, on which the nanotubes were deposited. The Si wafer was placed in the middle of the third temperature zone (deposition zone). The system was also equipped with a system supplying carrier gases—Ar (1 SLPM, Standard Liter Per Minute, 1 SLPM = 1.68875 Pa·m³/s) and H₂ (0.2 SLPM), and a precise system dosing the reaction substrate—Medima S2 pump. The reaction substrate was a ferrocene-xylene mixture (concentration 0.2 g/mL). Ferrocene was the source of iron, which was the ferromagnetic filling of the nanotubes and at the same time was the catalyst of the reaction. Xylene from Chempur and ferrocene from Sigma-Aldrich (U.S. company, Burlington, MA, USA) were used to prepare the solution. The solution was dispensed at a rate of 16 mL/h. The temperature in the evaporation zone was 175–325 °C, and in the deposition zone it was 750–850 °C [19,27].

These CNTs were purified thermally and chemically with a 5M solution of hydrogen chloride in order to remove the catalyst residues and amorphous carbon-based impurities. The iron content when examined was around 15% (Figure 2). The content was measured using thermogravimetric analysis (TGA) and then the remaining material was examined on the SEM-EDS examination. The result of TGA analysis shows also that fabricated CNTs were mostly multi-walled CNTs. Obtained material was also examined with XRD. According to the results, the iron content of CNTs consisted of α -Fe and γ -Fe phases. The presence of the α -Fe and γ -Fe phases was revealed by the observation diffraction peaks corresponding to the 111 reflection of γ -Fe and to the 110 reflection of α -Fe, respectively. The iron content was estimated to be 68% of the γ -Fe phase and 32% of the α -Fe phase. Fe₃C was not observed in the samples.

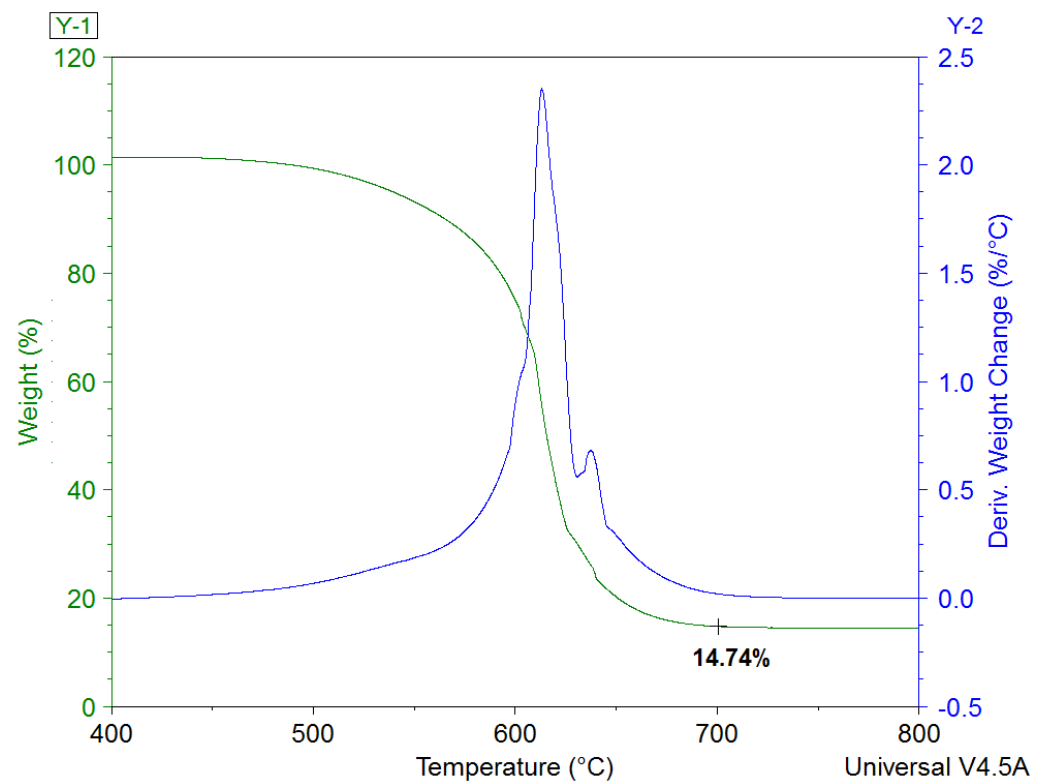


Figure 2. Thermogravimetric analysis of CNTs.

2.2. Experimental Setup

In order to investigate the heating quality of Fe and Fe-MWCNTs and to determine their magnetic properties, measurements of the temperature rise of magnetic fluids after exposure to an electromagnetic field of three frequencies (110.2 kHz, 168.5 kHz, and 329 kHz) were carried out. The studies were designed to compare the results using different concentrations in different suspensions.

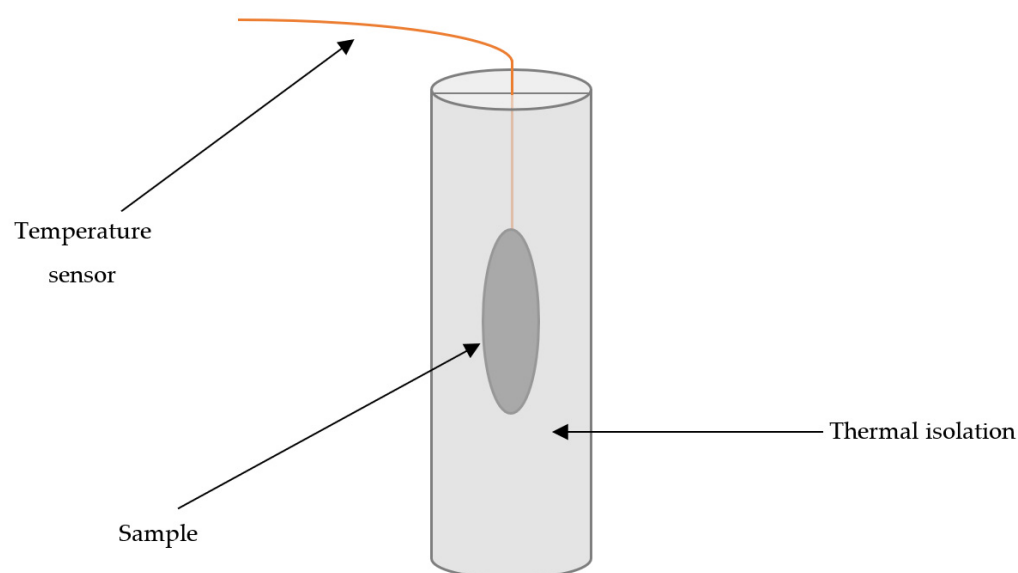
The first step of the process was the CNT sample preparation. In each sample, three ingredients were mixed together: CNTs, Sodium Lauryl Sulfate (SLS/SDS), and distilled water. The ratio of substrates of each sample and their concentrations are presented in Table 1. The ratio of CNTs to SDS should be approximately 1:2. The mixture of these 3 ingredients was then put in an ultrasound machine for 30 min. The ultrasound influence (combined with SDS) aimed to obtain a dispersion of CNTs in the sample. After half an hour, the sample was left for some time to cool down to room temperature. The last step was the insertion of the prepared sample into the nanotherics magneTherm, setting of appropriate parameters—frequency, voltage and current—and measurement using the SoftSens program.

The samples of magnetic suspension in Eppendorf were placed in polystyrene thermal insulation in a specialized heating device. All measurements were performed in a constant parameter environment with an initial measurement temperature of 25 °C. In addition, all temperature measurements were performed using a fiber optic temperature sensor to reduce the influence of the electromagnetic field on the temperature measurements. The exact location of the test samples is shown in the figure below (Figure 3).

The preparation of all samples of CNTs used for the examination is shown in Table 1.

Table 1. The ratio of components in samples with CNTs.

Sample No.	CNTs (mg)	SDS (mg)	Distilled Water (mL)	Concentration CNTs to H ₂ O (mg/mL)	Frequency (kHz)
1	15	30	4.0	3.75	110.2
2	15	30	2.0	7.50	110.2
3	15	30	1.0	15.00	110.2
4	15	30	0.5	30.00	110.2
5	15	30	4.0	3.75	168.5
6	15	30	2.0	7.50	168.5
7	15	30	1.0	15.00	168.5
8	15	30	0.5	30.00	168.5
9	15	30	4.0	3.75	329.0
10	15	30	2.0	7.50	329.0
11	15	30	1.0	15.00	329.0
12	15	30	0.5	30.00	329.0

**Figure 3.** Scheme of the placement of the fiber optic sensor, test tube, and polystyrene thermal insulation used during the temperature measurements.

3. Results

Firstly, the measurements were conducted at the frequency of 110.2 kHz. As the legend on the right of Figure 4 shows, four samples of different concentrations were considered. One can observe that the highest temperature rise was obtained in the case of sample no. 4 of the highest concentration from the four considered.

The observation drawn from the plots is that the tendency of temperature change was directly proportional to the concentration. With the increasing concentration, the temperature change also rises. It is clearly visible that it occurs respectively, as could be expected. Samples in the concentration of 3.75 mg/mL gain a temperature rise of only 0.5 °C. In the case of 7.5 mg/mL, the temperature change is higher and equals 1.5 °C. For 15 mg/mL, it was almost 3 °C and for the highest concentration of 30 mg/mL, the change was equal to approximately 5 °C.

Figure 5 depicts measurements in the frequency of 168.5 kHz. Similarly to Figure 4, four measurements were conducted (four different concentrations).

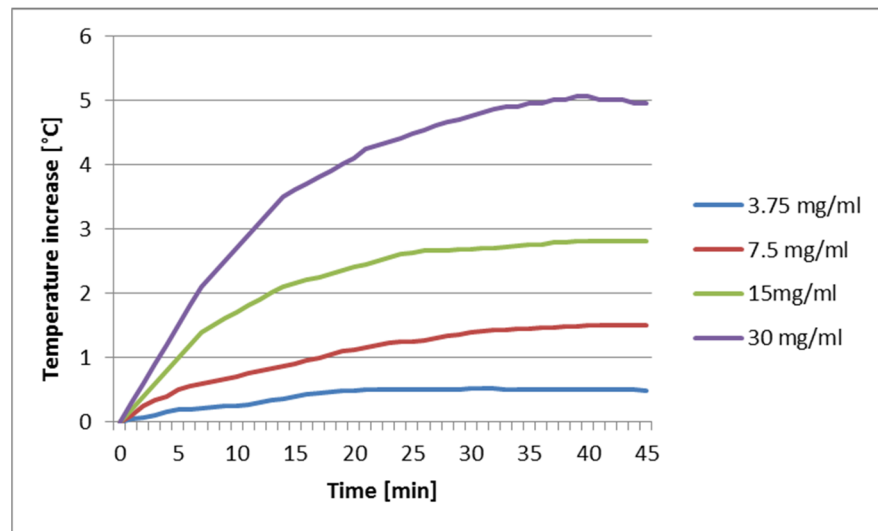


Figure 4. Plots of temperature change in time of samples 1–4 in frequency 110.2 kHz.

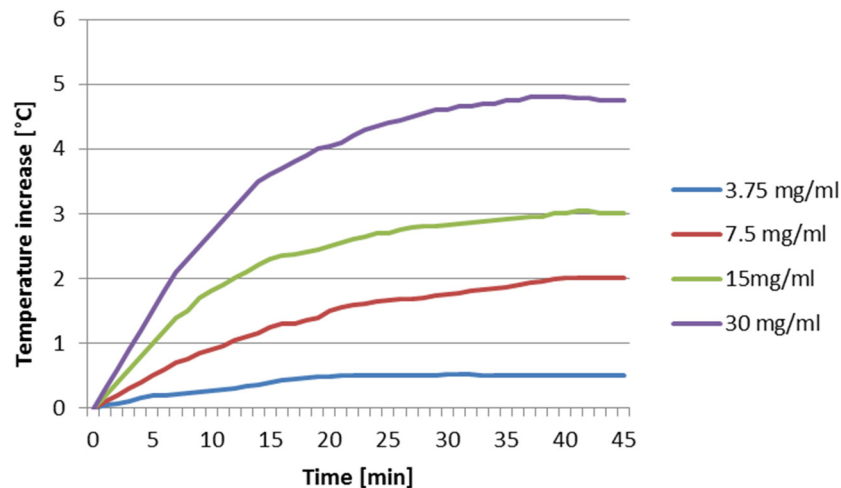


Figure 5. Plots of temperature change in time of samples 5–8 in frequency 168.5 kHz.

The same as at the frequency of 110.2 kHz, a higher concentration proved to gain a higher temperature. The heating of the sample in the concentration of 3.75 mg/mL did not result in almost any higher temperature, its temperature again rose by only a half-degree Celsius. For the sample of 7.5 mg/mL, the temperature was equal to around 2 °C. In the case of 15 mg/mL, it was around 3 °C. For the highest concentration of 30 mg/mL, the temperature rise was around 4.8 °C. The sample with the highest concentration also had a relatively quick change during the first 25 min. The same situation occurred for the concentration of 15 mg/mL, but for a shorter time period of 15 min.

Figure 6 shows the heating progression for the frequency of 329 kHz. Again, samples of the four concentrations are used in measurements.

This specific graph shows a time frame of 55 min. Thanks to that, further behavior can be observed. Worth noting is sample no. 12 of a concentration of 30 mg/mL. It exhibited the best heating properties compared to the other three samples. The tendency of direct proportionality between temperature change and time also occurs for this frequency. It is interesting that when comparing samples of concentrations 7.5 mg/mL and 15 mg/mL, the sample of lower concentration had a larger heating rate for the first 7 min. After that time, the sample of lower concentration flattens a bit, while the plot of the other keeps increasing. The sample with the concentration of 3.75 mg/mL heated up by approximately 1 °C and the sample of 7.5 mg/mL by approximately 2.3 °C. For 15 mg/mL, the rise was around 3.5 °C. In the case of 30 mg/mL, the temperature change equals almost 6 °C. An observation worth

mentioning is the trend of three of the plots—30 mg/mL, 15 mg/mL, and 3.75 mg/mL. As can be seen, these plots after reaching their peaks start to decrease. Nonetheless, these maximum values are reached in different time periods for each of the concentrations.

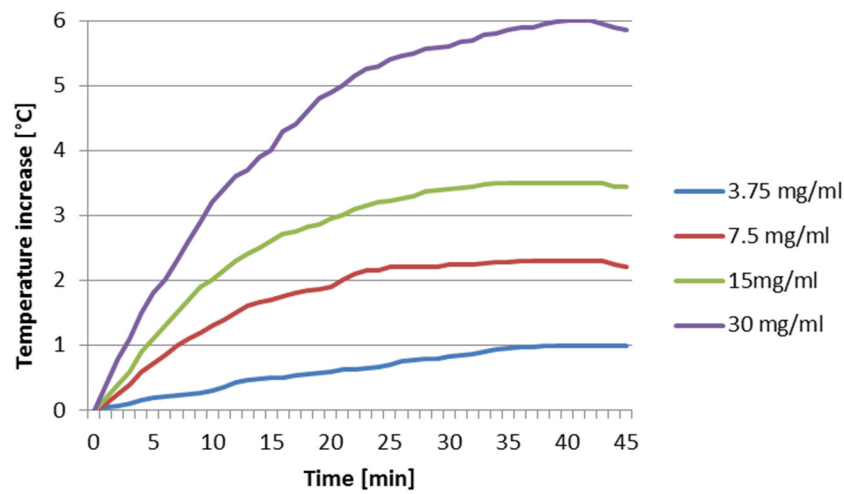


Figure 6. Plots of temperature change in time of samples 9–12 in frequency 329 kHz.

Below (Figure 7), all of the results obtained from measurements were gathered together. However, only the maximum values were depicted in order to show which sample proved to be the most efficient.

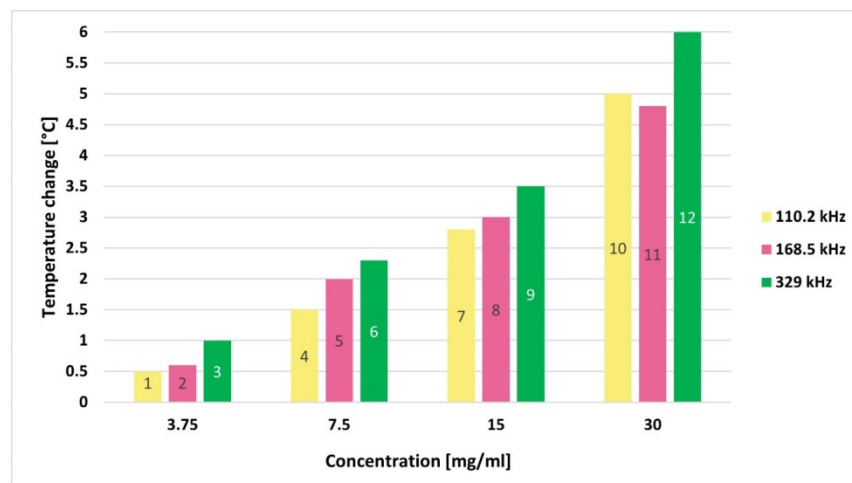


Figure 7. Bar chart of all measurements.

4. Discussion

The main aim of this work was an observation of the behavior of CNTs when influenced by a radiofrequency electromagnetic field and possibly finding the best conditions for the greatest heating rate. All the measurements had the most similar conditions as possible each of the times. Sometimes due to the observed heating rate, the measurements were shorter, hence various time periods in graphs.

The highest result obtained from all of the conducted tests was sample no. 12, which had a temperature increase of 6 °C. It was a sample of a concentration of 30 mg of CNTs per 1 mL of water in an electromagnetic field at a frequency of 329 kHz. The conditions of this measurement confirmed the original and most instinctive assumption. It was assumed that when the nanoparticles of iron inside the CNTs are the material that heats up, so with its higher concentration, the temperature change will also increase. Exactly as presumed, the higher concentrations of CNTs in the samples proved to gain larger temperature change. In all three EMF frequencies, the best results were obtained for the highest concentrations.

However, the concentrations were entirely dependent on the amount of components in each sample. Even though further increasing the concentration would logically provide better results, the main problem would be consistency. There were two attempts at preparing samples of a concentration of 60 mg/mL. Unfortunately, they were so dense that proper mixing of the components to obtain even distribution was very troublesome. Due to that, the measurements conducted on those two samples were not reliable enough. The general pattern of behavior was that the higher the concentration, the more the temperature increased. The three best temperature changes were obtained from samples with the concentration of 30 mg/mL in all three frequencies, giving a temperature rise of 6 °C for the highest frequency, 5 °C for the lowest, and 4.8 °C for the middle frequency.

The second variable was the frequency of EMF influencing the sample. A logical assumption was that the higher frequency would induce a higher heating rate, which was also proven to be true. All of the tested frequencies brought to some extent satisfying results. The higher frequency always had the highest heating rate. Interestingly, in the case of the two lower frequencies, the results were not always as expected. Firstly, the difference between the temperature changes was much smaller than when comparing two higher frequencies, but that is a result of only 58 kHz in frequency difference, while for the other pair the frequency was almost doubled. Secondly, the trends for lower frequencies were not always constantly above one another.

The results obtained correspond with literature [28] conclusions considering the main assumptions, but also there is a slight inconsistency of the heating rate of CNTs when influenced by the electromagnetic field. Nevertheless, there were also tests including heating of iron nanoparticles alone [29] and those proved to be very successful in a very short time. This means the effectiveness of such therapy has potential and should be more efficient when modified correctly. However, it is worth noting that when using the iron nanoparticles alone, their concentration was 100%, while in the case of CNTs used in these measurements, the content of iron examined on TGA was only 15%. This leads to drawing a conclusion that CNTs with a higher content of iron should be produced for more satisfying results. Unfortunately, the process of synthesis of CNTs is so complex that finding adequate conditions for the production of perfect CNTs is basically impossible. Luckily, their functionalization and modification give hope for some enhancements in that matter, especially since the first and most important requirement when applying it in human therapy is its biocompatibility and non-toxicity.

Even though the temperature in the results might not seem to increase significantly, one could conclude that 6 °C at certain conditions could be almost enough. One has to take into consideration that this compound is ultimately planned to be injected into the human body. Therefore, the starting temperature would be the human body temperature, which equals 36.6 °C. When heated to 42–43 °C, the cells get closer to the coagulation threshold.

5. Conclusions

The main problem encountered during the experiments so far has been found to be the uniform dispersion of the iron-filled carbon nanotubes. Before each measurement, each sample was mechanically dispersed. However, the physical properties of CNTs affected the rapid deposition of particles, which may have affected the results. Nevertheless, the results provide valuable information and a good reference for future research. One of the goals is to develop an effective dispersion method to further investigate the heating properties of the suspension at a given concentration and to begin cell line studies. In this phase, it will be necessary to estimate the number of nanocarriers used in the therapy to effectively destroy cells and to determine the exact field parameters used in the proposed method.

In conclusion, the results of this research have proven that with the increasing concentration of CNTs and increasing frequency, the heating rate increases as well. Unfortunately, it was mostly quite low or even non-existent in some of the trials. One also must take into account that the optic sensor used in the measurements was so sensitive, that its slightly improper placement could alter the final result to some extent. Nonetheless, the results

have proved that this method possesses a potential for such therapy with CNTs as the temperature of the samples was increasing. Unfortunately, some of the measurements have shown that the heating rate has its limits. In some cases, the temperature reached its maximum and started to decrease, despite unchanged conditions, which means that probably each type has its limitations that possibly could be neglected when improved. Another problem is that there is no standardization concerning the process of synthesis or specific composition or content of compounds. Therefore, considering that the application of CNTs in medicine could be the future of cancer treatment, first, there have to be general standards that could be applied by every laboratory and research center for further investigation.

The work aimed at producing ferromagnetic nanoparticles encapsulated in carbon nanotubes, making them safe for medical applications due to the external carbon. The produced material was examined with the XRD studies, in the research a spectrum corresponding to iron was registered. The presence of the α -Fe and γ -Fe phases was observed. Due to the limited time available, it was not possible to go into the subject of disposing of the γ -Fe phase. α -Fe is widely considered to be one of the most promising magnetic phases that can be encapsulated internally within CNTs in the form of continuous nanowires. Fortunately, the XRD examination showed the presence of this phase and consequently this confirms the existence in the sample of magnetic iron filling the carbon nanotubes. Work on improving the material, and to obtain more of the α -Fe phase as the content of carbon nanotubes, is currently in progress.

The results obtained during this experiment provide valuable information which is a good reference for further research. In future experiments, an effective method for dispersing of iron powder in solvent should be verified. Achieving this goal will allow for a detailed characterization of the heating properties of the suspension. Based on this knowledge, it will be possible to determine the field parameters necessary for the therapy. Successful completion of this phase is essential and opens the door to in vitro studies. In this phase, the amount and concentration of nanoparticles suspended in the biocompatible solution must be determined and the exposure parameters well defined to focus on the response of the cells to the heating medium.

Author Contributions: Conceptualization, K.W. and Ł.S.; methodology, K.W. and A.U.; investigation, K.W. and A.U.; writing—original draft preparation, K.W. and A.U.; writing—review and editing, K.W., K.S. and Ł.S.; visualization, K.W., A.U. and K.S.; supervision, Ł.S. and S.W. All authors have read and agreed to the published version of the manuscript.

Funding: This research received no external funding.

Institutional Review Board Statement: Not applicable.

Informed Consent Statement: Not applicable.

Data Availability Statement: Not applicable.

Conflicts of Interest: The authors declare no conflict of interest.

References

1. Poudel, Y.R.; Li, W. Synthesis, properties, and applications of carbon nanotubes filled with foreign materials: A review. *Mater. Today Phys.* **2018**, *7*, 7–34. [[CrossRef](#)]
2. Long, R.Q.; Yang, R.T. Carbon Nanotubes as Superior Sorbent for Dioxin Removal. *J. Am. Chem. Soc.* **2001**, *123*, 2058–2059. [[CrossRef](#)]
3. Jang, H.G.; Yang, B.; Khil, M.-S.; Kim, S.Y.; Kim, J. Comprehensive study of effects of filler length on mechanical, electrical, and thermal properties of multi-walled carbon nanotube/polyamide 6 composites. *Compos. Part A Appl. Sci. Manuf.* **2019**, *125*, 105542. [[CrossRef](#)]
4. Bellucci, S.; Balasubramanian, C.; Micciulla, F.; Rinaldi, G. CNT composites for aerospace applications. *J. Exp. Nanosci.* **2007**, *2*, 193–206. [[CrossRef](#)]
5. Maheswaran, R.; Shanmugavel, B.P. A Critical Review of the Role of Carbon Nanotubes in the Progress of Next-Generation Electronic Applications. *J. Electron. Mater.* **2022**, *51*, 2786–2800. [[CrossRef](#)]
6. He, J.; Xu, P.; Zhou, R.; Li, H.; Zu, H.; Zhang, J.; Qin, Y.; Liu, X.; Wang, F. Combustion Synthesized Electrospun InZnO Nanowires for Ultraviolet Photodetectors. *Adv. Electron. Mater.* **2021**, *8*, 2100997. [[CrossRef](#)]

7. Daneshvar, F.; Chen, H.; Noh, K.; Sue, H.-J. Critical challenges and advances in the carbon nanotube–metal interface for next-generation electronics. *Nanoscale Adv.* **2021**, *3*, 942–962. [[CrossRef](#)]
8. Jamali, V.; Niroui, F.; Taylor, L.; Dewey, O.S.; Koscher, B.A.; Pasquali, M.; Alivisatos, A.P. Perovskite–Carbon Nanotube Light-Emitting Fibers. *Nano Lett.* **2020**, *20*, 3178–3184. [[CrossRef](#)]
9. Kwo, J.; Yokoyama, M.; Wang, W.; Chuang, F.; Lin, I. Characteristics of flat panel display using carbon nanotubes as electron emitters. *Diam. Relat. Mater.* **2000**, *9*, 1270–1274. [[CrossRef](#)]
10. Siraj, N.; Macchi, S.; Berry, B.; Viswanathan, T. Metal-Free Carbon-Based Supercapacitors—A Comprehensive Review. *Electrochem* **2020**, *1*, 410–438. [[CrossRef](#)]
11. Takagi, D.; Homma, Y.; Hibino, H.; Suzuki, A.S.; Kobayashi, Y. Single-Walled Carbon Nanotube Growth from Highly Activated Metal Nanoparticles. *Nano Lett.* **2006**, *6*, 2642–2645. [[CrossRef](#)] [[PubMed](#)]
12. Zhang, J.; Liu, S.; Kong, L.; Nshimiyimana, J.P.; Hu, X.; Chi, X.; Wu, P.; Liu, J.; Chu, W.; Sun, L. Room-Temperature Carbon Nanotube Single-Electron Transistors with Mechanical Buckling-Defined Quantum Dots. *Adv. Electron. Mater.* **2018**, *4*, 2036. [[CrossRef](#)]
13. Kaushik, B.K.; Majumder, M.K. *Carbon Nanotube Based VLSI Interconnects*; Springer India: New Delhi, India, 2015. [[CrossRef](#)]
14. Jorio, A.; Dresselhaus, G.; Dresselhaus, M.S. *Carbon Nanotubes: Advanced Topics in the Synthesis, Structure, Properties and Applications*; Springer: Berlin/Heidelberg, Germany, 2007.
15. Saito, N.; Haniu, H.; Usui, Y.; Aoki, K.; Hara, K.; Takanashi, S.; Shimizu, M.; Narita, N.; Okamoto, M.; Kobayashi, S.; et al. Safe Clinical Use of Carbon Nanotubes as Innovative Biomaterials. *Chem. Rev.* **2014**, *114*, 6040–6079. [[CrossRef](#)] [[PubMed](#)]
16. Guo, Q.; Shen, X.-T.; Li, Y.-Y.; Xu, S.-Q. Carbon nanotubes-based drug delivery to cancer and brain. *Curr. Med. Sci.* **2017**, *37*, 635–641. [[CrossRef](#)] [[PubMed](#)]
17. Raza, K.; Kumar, D.; Kiran, C.; Kumar, M.; Guru, S.K.; Kumar, P.; Arora, S.; Sharma, G.; Bhushan, S.; Katare, O.P. Conjugation of Docetaxel with Multiwalled Carbon Nanotubes and Codelivery with Piperine: Implications on Pharmacokinetic Profile and Anticancer Activity. *Mol. Pharm.* **2016**, *13*, 2423–2432. [[CrossRef](#)]
18. Martincic, M.; Tobias, G. Filled carbon nanotubes in biomedical imaging and drug delivery. *Expert Opin. Drug Deliv.* **2014**, *12*, 563–581. [[CrossRef](#)]
19. Wojtera, K.; Walczak, M.; Pietrzak, L.; Fraczyk, J.; Szymanski, L.; Sobczyk-Guzenda, A. Synthesis of functionalized carbon nanotubes for fluorescent biosensors. *Nanotechnol. Rev.* **2020**, *9*, 1237–1244. [[CrossRef](#)]
20. Bhirde, A.A.; Patel, V.; Gavard, J.; Zhang, G.; Sousa, A.A.; Masedunskas, A.; Leapman, R.D.; Weigert, R.; Gutkind, J.S.; Rusling, J.F. Targeted Killing of Cancer Cells in Vivo and in Vitro with EGF-Directed Carbon Nanotube-Based Drug Delivery. *ACS Nano* **2009**, *3*, 307–316. [[CrossRef](#)]
21. Chen, D.; Wang, C.; Nie, X.; Li, S.; Li, R.; Guan, M.; Liu, Z.; Chen, C.; Wang, C.; Shu, C.; et al. Photoacoustic Imaging Guided Near-Infrared Photothermal Therapy Using Highly Water-Dispersible Single-Walled Carbon Nanohorns as Theranostic Agents. *Adv. Funct. Mater.* **2014**, *24*, 6621–6628. [[CrossRef](#)]
22. Antaris, A.L.; Robinson, J.T.; Yaghi, O.K.; Hong, G.; Diao, S.; Luong, R.; Dai, H. Ultra-Low Doses of Chirality Sorted (6,5) Carbon Nanotubes for Simultaneous Tumor Imaging and Photothermal Therapy. *ACS Nano* **2013**, *7*, 3644–3652. [[CrossRef](#)]
23. Zhang, M.; Wang, W.; Wu, F.; Yuan, P.; Chi, C.; Zhou, N. Magnetic and fluorescent carbon nanotubes for dual modal imaging and photothermal and chemo-therapy of cancer cells in living mice. *Carbon* **2017**, *123*, 70–83. [[CrossRef](#)]
24. Murakami, T.; Nakatsuji, H.; Inada, M.; Matoba, Y.; Umeyama, T.; Tsujimoto, M.; Isoda, S.; Hashida, M.; Imahori, H. Photodynamic and Photothermal Effects of Semiconducting and Metallic-Enriched Single-Walled Carbon Nanotubes. *J. Am. Chem. Soc.* **2012**, *134*, 17862–17865. [[CrossRef](#)] [[PubMed](#)]
25. Samali, A.; Holmberg, C.I.; Sistonen, L.; Orrenius, S. Thermotolerance and cell death are distinct cellular responses to stress: Dependence on heat shock proteins. *FEBS Lett.* **1999**, *461*, 306–310. [[CrossRef](#)]
26. Roti, J.L.R. Cellular responses to hyperthermia (40–46 °C): Cell killing and molecular events. *Int. J. Hyperth.* **2008**, *24*, 3–15. [[CrossRef](#)] [[PubMed](#)]
27. Szymanski, L.; Kolacinski, Z.; Wiak, S.; Raniszewski, G.; Pietrzak, L. Synthesis of Carbon Nanotubes in Thermal Plasma Reactor at Atmospheric Pressure. *Nanomaterials* **2017**, *7*, 45. [[CrossRef](#)]
28. Singh, R.; Torti, S.V. Carbon nanotubes in hyperthermia therapy. *Adv. Drug Deliv. Rev.* **2013**, *65*, 2045–2060. [[CrossRef](#)]
29. Pazouki, N.; Irani, S.; Olov, N.; Atyabi, S.M.; Bagheri-Khoulenjani, S. Fe₃O₄ nanoparticles coated with carboxymethyl chitosan containing curcumin in combination with hyperthermia induced apoptosis in breast cancer cells. *Prog. Biomater.* **2022**, *11*, 43–54. [[CrossRef](#)]